arXiv:1512.06215v2 [nucl-th] 15 Jul 2016

The effect of momentum deposition during fireball evolution on flow anisotropy

Martin Schulc[1,2] **and Boris Tomášik**[1,3]

[1]Czech Technical University in Prague, FNSPE, 11519 Prague, Czech Republic
[2]Research Centre Řež, 25068 Husinec-Řež, Czech Republic
[3]Univerzita Mateja Bela, Fakulta prírodných vied, 97401 Banská Bystrica, Slovakia

E-mail: martin.schulc@cvrez.cz

Abstract. The highest LHC energies give rise to production of many pairs of hard partons which deposit four-momentum into the expanding fireball matter. We argue that it is necessary to include momentum deposition during fireball evolution into 3+1 dimensional hydrodynamic simulations of the collision. This influence cannot be accounted for simply by modifying initial conditions of the simulation. The resulting contribution to flow anisotropy is correlated with the fireball geometry and causes an increase of the elliptic flow in non-central collisions. The results are presented for various scenarios with energy and momentum deposition to clearly demonstrate this effect.

PACS numbers: 25.75.-q, 25.75.Bh, 25.75.Ld

1. Introduction

The goal of high-energy heavy-ion collisions is to study properties of matter in deconfined state. Relativistic hydrodynamics has proven to be very successful tool for modelling the bulk dynamics of the hot dense matter formed during a heavy ion collision [1, 2, 3, 4, 5, 6]. Comparisons of hydrodynamic simulations with the measured data aim at extracting the equation of state (EoS) and the transport coefficients, such as the shear and bulk viscosities. The importance of including fluctuations into hydrodynamic calculations has been recognized, leading to a new set of experimental observations of higher flow coefficients and their correlations [7, 8, 9, 10]. Event-by-event viscous hydrodynamic modelling has proven to be essential for correctly describing all the details of the bulk behaviour of heavy ion collisions. The standard approach being used now is to select a set of initial conditions and to tune the values of transport coefficients in order to find such a setting of hydrodynamic simulations which reproduces all features of the data. Simulations indicate linear mapping of initial state spatial anisotropies onto final state momentum distribution anisotropies on event-by-event basis [11, 12, 13]. The mechanism, that is being investigated here, breaks such a direct correspondence.

It has been demonstrated that at the LHC energy, momentum deposition from hard partons into expanding matter effectively produces measurable anisotropy in transverse expansion [14, 15, 16]. Here we show that the effect cannot be simulated by just including momentum anisotropies into initial conditions. Jets and minijets are produced copiously in initial hard scatterings at the highest achievable energies at the LHC and propagate through the deconfined medium. The quark-gluon plasma extensively quenches the energy and momentum carried by hard partons which might become jets. Their energy loss when traversing the matter is so huge that only a few of them appear as distinguished jets [17, 18, 19, 20]. The momentum and energy depositions from partons into bulk medium induce collective phenomena there [21, 22, 23]. The approach presented in this paper bears two distinctive features. Firstly, energy loss is accompanied by deposition of momentum directed along the hard parton motion. Secondly, it is being deposited over some period of time and not just instantaneously at the beginning of the expansion.

In our previous work [14] we have shown that the interplay of many hard-partons-induced streams in a single nuclear collision at the LHC yields considerable contribution to azimuthal anisotropies of hadron distributions. In non-central collisions the contribution is correlated with fireball geometry. Surprisingly, it was found that the magnitude of this effect does not significantly depend on the value of dE/dx, at least for the two tested values of the energy loss. This triggers the question whether the effect on flow anisotropies would not be the same if all energy and momentum were deposited in the initial conditions. The argument favouring such a conclusion might be that the total amount of deposited energy and momentum is always the same, and a higher value of dE/dx only means that it is deposited faster. The case which includes energy and momentum deposition in initial conditions actually corresponds to an infinite value of dE/dx. In the present paper it will be compared with scenarios where energy-momentum is deposited during evolution of the fireball. We show that including momentum and energy deposition only in the initial stage is not enough to create azimuthal anisotropy of the same size as in case with deposition during the evolution of the fireball.

We also investigate more fine-tuning details of the scenario with energy and momentum deposition *during* the hydrodynamic evolution. Our conclusions appear robust against reasonable changes of the model parameters.

The paper is organised as follows. Section 2 introduces the methods and ideal three-dimensional hydrodynamic model that was used in our simulations. Then, Section 3 presents our results obtained with this model for the simulation of energy and momentum deposition from pairs of hard partons in different configurations. Important conclusions are summarised in Section 4.

2. Calculation methods

To simulate the energy-momentum deposition from hard partons at the beginning or during the evolution of the fireball we have employed ideal event-by-event three-dimensional hydrodynamic model. It uses the SHASTA algorithm [32, 33] to treat

strong gradients and shocks without dispersion.

The initial conditions are calculated by means of smooth optical Glauber prescription. We have chosen these simple initial conditions since any contribution of hard partons generates distinct features over this background and can be easily distinguished. By using different initial conditions as *e.g.* Glauber Monte Carlo, distinction of hard partons effect would be very hard or almost impossible. The nucleon-nucleon cross-section for Glauber calculation at $\sqrt{s_{NN}} = 5.5$ TeV was set to 62 mb. The shape of initial energy density distribution in the transverse plane is parametrized as

$$W(x, y; b) = (1 - \alpha) n_w(x, y; b) + \alpha n_{bin}(x, y; b), \tag{1}$$

where n_w and n_{bin} are the numbers of wounded nucleons and binary collisions at given transverse position (x, y) and the coefficient α which determines the fraction of the binary collisions contribution was set to 0.16. For the longitudinal profile we employed the prescription used in [2, 27]. It consists of two parts, a flat region around $\eta_s = 0$ and half-Gaussian in the forward and backward end of the plateau:

$$H(\eta_s) = \exp\left[-\frac{(|\eta_s| - \eta_{flat}/2)^2}{2\sigma_\eta^2}\theta(|\eta_s| - \eta_{flat}/2)\right]. \tag{2}$$

The parameters $\eta_{flat} = 10$ and $\sigma_\eta = 0.5$ were chosen according to [28]. The complete energy density distribution is then given by

$$\epsilon(x, y, \eta_s, b) = \epsilon_0 H(\eta_s) \frac{W(x, y, b)}{W(0, 0, 0)}. \tag{3}$$

We choose $\epsilon_0 = 60$ GeV/fm^3 and the initial proper time τ_0 was set to 0.55 fm.

The initial expansion velocity field was longitudinally boost invariant without any transverse component. This was modified only in the hotspots-with-momentum model, as we explain below.

To close the hydrodynamic set of equations we employed a lattice-inspired nuclear equation of state [29].

Incorporation of energy and momentum deposition due to hard partons into hydrodynamic equations was done via source terms in the energy-momentum conservation equation

$$\partial_\mu T^{\mu\nu}(x) = J^\nu, \tag{4}$$

where $T^{\mu\nu}(x)$ is the energy-momentum tensor and the term J^ν on the right-hand side is the parametrised source term describing deposition of energy and momentum into the medium [30, 31]

$$J^\nu = -\sum_i \int_{\tau_i,i}^{\tau_f,i} d\tau \frac{dP_i^\nu}{d\tau} \delta^{(4)}(x^\mu - x_{jet,i}^\mu), \tag{5}$$

where $x_{jet,i}^\mu$ denotes the position of i-th hard parton and $dP_i^\mu/d\tau$ is its momentum change. Integration runs over the whole lifetime of i-th parton until its energy is fully deposited and the summation goes over all hard partons of the event. Their source term

is in non-covariant notation implemented in a form of a three-dimensional Gaussian function in x, y and η coordinates [14, 24, 30]

$$J^j = -\sum_i \frac{1}{(2\,\pi\,\sigma_i^2)^{\frac{3}{2}}}\,\exp\left(-\frac{(\vec{x}-\vec{x}_{jet,i})^2}{2\,\sigma_i^2}\right)\,\left(\frac{dE_i}{dt},\frac{d\vec{P}_i}{dt}\right)\,. \tag{6}$$

The sum runs over all the jets and the Gaussian profiles are centered around the actual positions of the partons. The width of the Gaussians σ_i was set to 0.3 fm as in [14]. We have checked that tuning the width to 0.15 fm or to 0.6 fm does not lead to major change of our results.

Since it is more suitable for the nature of the problem, hydrodynamic simulations have been performed in Milne coordinates $\eta = \frac{1}{2}\ln((t+z)/(t-z))$ and $\tau = \sqrt{t^2-z^2}$. The formulation of the source term has been adjusted accordingly in the numerical procedure. They are evolved in proper time, as indicated in Eq. (5). The widths which appear in Eq. (6) refer to Cartesian coordinates and cannot be used for η without any change. Indeed, in order to keep constant longitudinal width for the energy deposition, the width in η has been scaled by τ^{-1}.

Parton energy loss depends on the density of the surrounding medium. We assume that parton energy loss scales with entropy density as in [34]. The scaling relation is then

$$\frac{dE}{dx} = \left.\frac{dE}{dx}\right|_0 \frac{s}{s_0} \tag{7}$$

with s_0 corresponding to energy density 20.0 GeV/fm^3 ($T = 324$ MeV with the used EoS). This gives $s_0 = 78.2/\mathrm{fm}^3$. For $dE/dx|_0$ we usually choose the value 7 GeV/fm in this paper. We have also made simlations, however, with very low dE/dx in order to study the limit of vanishing energy loss.

For the production of hard partons we take the parametrisation of gluon cross-section per nucleon-nucleon pair in nucleus-nucleus collisions from [35]

$$E\frac{d\sigma_{NN}}{d^3p} = \frac{1}{2\pi}\frac{1}{p_t}\frac{d\sigma_{NN}}{dp_t dy} = \frac{B}{(1+p_t/p_0)^n}, \tag{8}$$

where for the energy $\sqrt{s_{NN}} = 5.5\,\mathrm{TeV}$ we have $B = 14.7\ \mathrm{mb/GeV^2}$, $p_0 = 6$ GeV and $n = 9.5$. This equation describes the initiation of hard partons in our hydrodynamic model at τ_0. Pairs of hard partons are generated back-to-back in transverse momentum with directions chosen in azimuthally symmetric manner. Thus the transverse momentum is always conserved for each pair of hard partons. Rapidities of the hard partons are generated from a uniform distribution and they are chosen independently for both partons of a pair.

The starting distribution of hard parton pairs in transverse plane scales with the number of binary collisions. Initial positions in η are chosen from uniform distribution. For the presented results we generated partons with p_t above 3 GeV. Altogether this procedure spits in average about 10 hard partons per central event into our simulation. More details of the whole procedure can be found in [14, 35].

Recorded freeze-out hypersurfaces given by $T = 150$ MeV were processed by the Cooper-Frye formula [36]. For every scenario recorded below we generated 100 hydrodynamic events. We use the THERMINATOR2 package [37] to generate observable hadrons on the obtained hypersurface and evaluate the results. For every hydrodynamic event there were five THERMINATOR2 events generated, thus giving 500 events in total for each setting. Resonance decays were included. Anisotropic flow parameters v_1, v_2, v_3, v_4 for charged hadrons were extracted by the two-particle cumulant method.

3. Results

The philosophy of our approach is to present the effect of any source of momentum anisotropy against the baseline given by simulation with smooth non-fluctuating optical Glauber initial conditions. Thus we always show such results which are marked "no-jets". We do so even if they are trivial as e.g. in the case of central collisions, also in order to validate our hydrodynamic model.

It is currently an open question, what is the value of $dE/dx|_0$. Surprisingly, in [14] we observed that the anisotropic flow coefficients did not change whether we chose 4 GeV/fm or 7 GeV/fm. Hence, it is interesting to investigate the limit case where $dE/dx|_0 \to \infty$. It corresponds to the case where momentum and energy is deposited in initial conditions. Exploration of this limiting case is important. If it leads to the same results as the simulations with finite dE/dx, then all inhomogeneities in energy and momentum density can be put into initial conditions. As a consequence, we would recover the linear relationship between initial state spatial anisotropy and final state distributions of hadrons [11, 12, 13]. If, on the other hand, energy and momentum deposition *during* the evolution leads to different results, then it must be properly included in phenomenologically relevant simulations.

Moreover, we considered the opposite limit, *i.e.* $dE/dx|_0 \to 0$. In our simulations, the value of dE/dx was set to 0.1 GeV/fm. The results for all anisotropic flow coefficients were found to be compatible with zero. The main reason is that the hydrodynamic simulation ends before significant amount of energy or momentum is deposited.

A little more on the technical side, we also investigated influence of varying the width of the deposited energy and momentum Gaussian for hard partons scenario. The change of the Gaussian width to 0.6 fm gives slightly higher values of anisotropic flow coefficients than results for 0.3 fm. Conversely, Gaussian width of 0.15 fm gives slightly lower values of flow coefficients. However, the results for all considered widths can be regarded approximately same within the error bars.

For our main investigation, we begin with the study of the generated anisotropy of momentum distribution in ultra-central collisions ($b = 0$) for various scenarios. Results are shown in Figure 1. Results of our model are represented by a set of "jet events" with $\frac{dE}{dx}\big|_0 = 7$ GeV/fm. As a benchmark test we also evaluate the v_n's from simulation with no hard partons and no fluctuations of the initial state and show that they are

consistent with 0.

In order to see if comparable results can be obtained with appropriately set initial conditions, we compare the results with simulations with hot-spots. Two versions of this scenario are investigated. In both cases the baseline smooth initial conditions are chosen according to eqs. (1–3). The hot-spots scenario refer to case where energy is superimposed on the smooth initial energy density profile. The hot-spots-with-momentum scenario refers to the case where energy as well as momentum are superimposed onto the baseline initial conditions. Energy and momentum anisotropy is completely included in the initial conditions and not released over the finite time interval. In these regions, the same amount of energy and momentum is deposited as a hard parton would carry if it was produced there. Also the number of hot spots corresponds to number of hard partons in simulations with hard partons. Their size is the same as would be the spatial spread of energy deposition from hard partons at the beginning of the hydrodynamic evolution. Positions of hot spots are chosen from the distribution, which is also the same as in the case with hard partons: *i.e.* it is the distribution of initial binary collisions. Additional momentum deposition also modifies

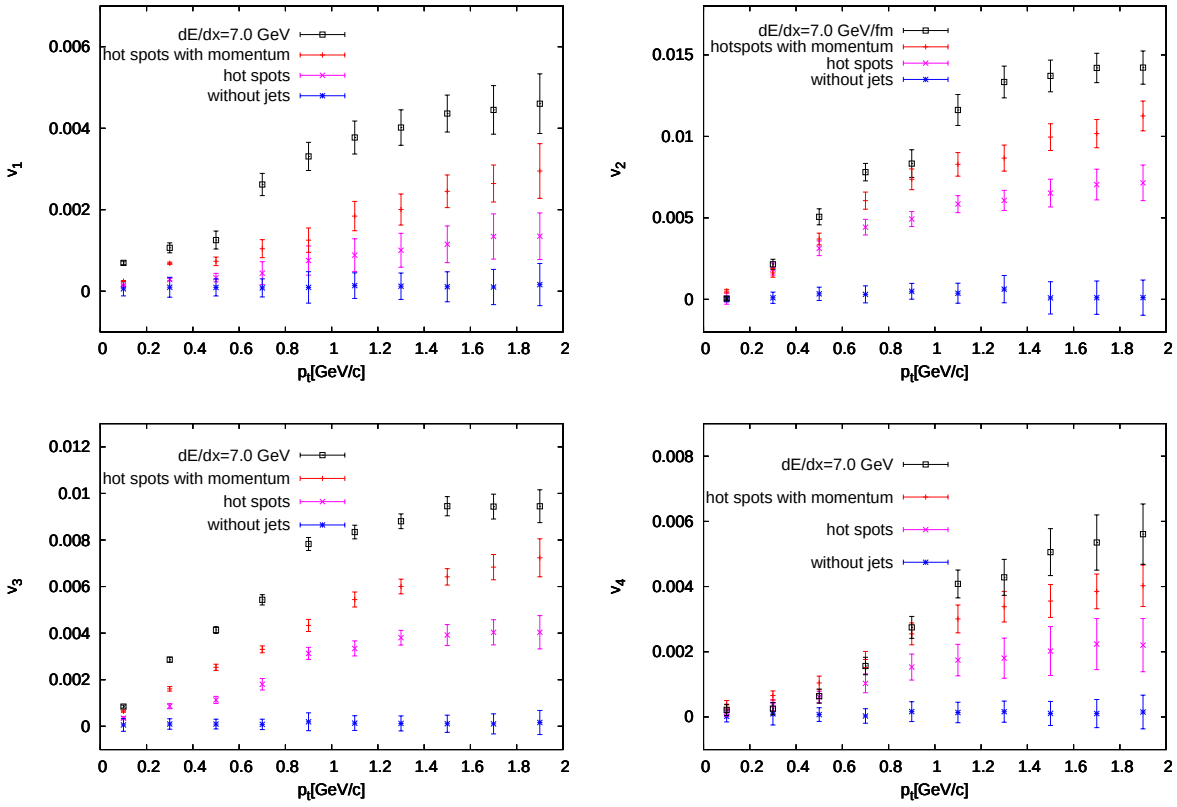

Figure 1. Parameters v_n from collisions at $b = 0$ for charged hadrons. Different symbols represent: energy loss of hard parton $dE/dx|_0 = 7$ GeV/fm (black □), scenario with hot spots with momentum deposition in initial conditions (red –), scenario with only hot spots in initial conditions (purple ×), and scenario with smooth initial conditions (blue *).

the initial expansion velocity field accordingly.

Comparison in Fig. 1 shows the importance of momentum deposition *during* the hydrodynamic evolution. It has been shown previously [14] that the hot-spots simulation does not produce the same amount of momentum anisotropy as the forces by which hard partons pull the plasma. Here, we show that neither fluctuations with momentum deposition in the initial conditions by themselves are able to generate the same flow anisotropies as wakes with streams induced by hard partons. Note that non-vanishing of v_1 is caused by transverse momentum of hard partons which have escaped the studied rapidity interval $\langle -1, 1\rangle$ and lead to the transverse momentum imbalance.

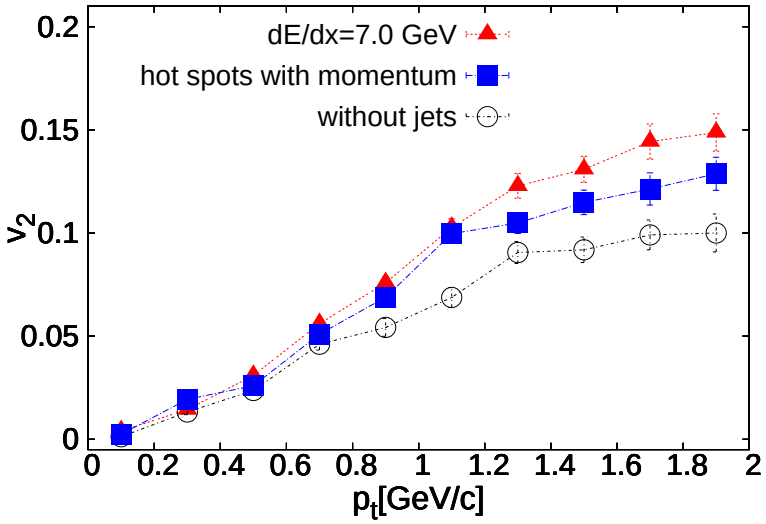

Figure 2. Anisotropy parameters v_2 for charged hadrons as functions of p_t from collisions within centrality class 30-40%. The energy loss of hard partons is given by $dE/dx|_0 = 7$ GeV/fm, other scenarios as in Fig. 1.

Next, we move further in centrality and simulate sets of events within centrality class 30–40% (b = 6–7 fm). Results for anisotropy coefficient v_2 are shown in Fig. 2. Similarly, results for v_3 are presented in Fig. 3. The results of v_2 demonstrate that the flow anisotropy generated by hard partons is correlated with the reaction plane. With hard partons added, v_2 grows by about 50% with respect to simulation with smooth initial conditions and no hard partons. Of course, v_3 vanishes in the absence of hard partons or hot spots due to the lack of third order anisotropy within the bulk matter.

Again here, we investigate whether the effect of energy-momentum deposition from hard partons can be represented by an appropriate choice of the initial conditions. In [14] we have shown that adding hot spots with energy deposition does not lead to the same effect as hard partons. Here, in Figs. 2 and 3 we show results of simulations with energy *and momentum* superposition onto the smooth profile of the initial conditions. Also here, the amount and distribution of energy and momentum is the same as would be carried by hard partons if they were integrated into the evolution. We observe that even the inclusion of hot spots with momentum into the initial state cannot account for

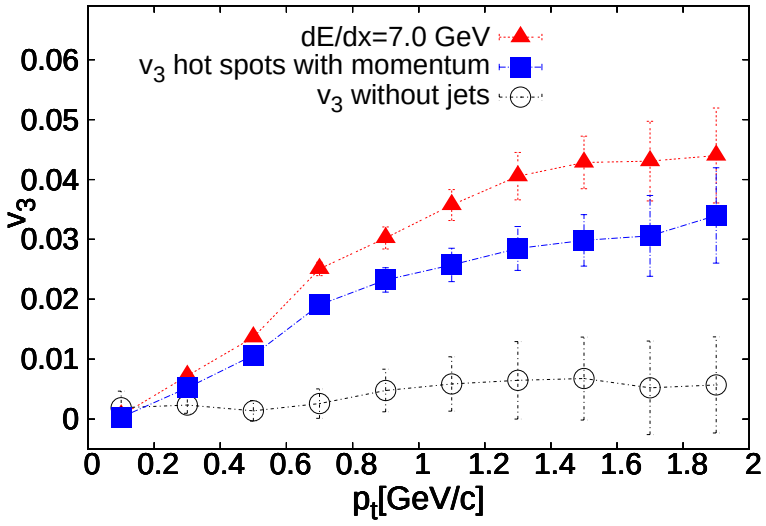

Figure 3. Anisotropy parameters v_3 for charged hadrons as functions of p_t from collisions within centrality class 30-40%. The energy loss of hard partons is given by $dE/dx|_0 = 7$ GeV/fm, other curves as in Fig. 2.

the whole effect on anisotropy which is generated by momentum deposition from hard partons during the evolution of the hydrodynamic bulk.

4. Summary and conclusions

Our results show that the momentum deposition during fireball evolution must be included in a realistic hydrodynamic simulation.

As a consequence, the linear relation between initial state anisotropies and v_n's may not be fully justified because in our suggested mechanism the anisotropy can rise during the fireball evolution. This is most clearly shown in our results for ultra-central collisions (Fig. 1). Initial state anisotropies of all orders vanish in those simulations.

We restricted our simulations here to the academic case with no fluctuations in the initial state of the hydrodynamic evolution. This allowed us to estimate the effect of momentum deposition from hard partons onto the resulting momentum anisotropies. The real quantitative influence can only be evaluated in complete simulations with initial state fluctuations. It might well be that the observed data on v_n's can be reproduced with suitably chosen initial conditions even if our mechanism is left out. However, the mechanism proposed here is quite natural and should be included. One should be careful in making conclusions about the initial state fluctuations based on simulations with our mechanism not included.

A related question is then posed: can one find a relevant measure of spatial fireball anisotropy which is then translated into final-state momentum anisotropy? Perhaps the evolution of anisotropy decomposition into orthogonal terms [38, 39] may provide some insights here.

Even more promising tool might be including femtoscopy among the methods to

analyse fireball dynamics. The v_n's can be caused by an anisotropy of the fireball in spatial shape and/or expansion pattern at the freeze-out. Both these effects cannot be determined uniquely just by analysis of single-particle distributions [40, 41, 42]. Fireball evolution with or without momentum deposition might end up in different spatial shapes even though they produce the same v_n's. Thus a complementary view might be obtained by looking at the azimuthal dependence of the femtoscopic correlation radii in second, third, and possibly higher orders [40, 41, 42]. Such an analysis has not been performed too often in experiments; only PHENIX collaboration has published results on third-order oscillations of correlation radii [43]. Perhaps one can even refrain from aligning the events to the second-order or the third-order event plane and use the method of Event Shape Sorting to select events so that oscillations to all orders can be studied together [44].

Figures 2 and 3 confirm the results obtained from ultra-central sets of events, that the interplay of many hard-partons-induced streams causes significant contribution to the azimuthal anisotropies. This cannot be replaced by initial-state-generated flow anisotropies.

It remains to explore the influence of viscosities and fluctuating initial conditions on anisotropic parameters for all presented scenarios. The effect of shear viscosity is the drag in case of velocity gradients transverse to the direction of the velocity. Therefore, the momentum which is transferred from the hard parton onto the fluid might spread into a broader stream. This is in line with the simulations of Mach cones in the partonic transport model BAMPS which reasonably resembles viscous 3+1-dimensional hydrodynamics [45, 46]. The broader streams would be more likely to interact. Recall that it is the interaction and merging of such streams which is crucial for the effect of aligning the flow anisotropy with the geometry of the collision [35]. Hence, surprisingly, viscosity can even amplify the momentum anisotropy observed.

We have not investigated the effect of different path dependence of the energy loss. Changing the types of path dependence (e.g. linear, quadratic, ...) would lead to changes of where the momentum is deposited during the hydrodynamic evolution. Since no visible variation of the resulting v_n's was observed when varying the absolute size of dE/dx within reasonable bounds, we do not expect much effect here either. The tool to distinguish various models might rather be the study of elliptic flow at high p_t which comes from hard partons that survived and fly out of the medium.

The ultimate goal will be to provide unified description of the momentum anisotropies in both low-p_t and high-p_t regimes. Such an attempt has been made with the help of parton energy loss model JEWEL [47, 48, 49]. It has been combined with hydrodynamical model but only the influence on the radial flow has been estimated to be low [50, 51], while here we were interested in flow anisotropies. (We have checked that the azimuthal angle-integrated single-particle spectra are hardly changed in our simulations, also.) Thus a part of the task is also to find the overlap with other models and compare individual models on the market.

Acknowledgements This work was partially supported by RVO68407700, LG15001 (Czech Republic), VEGA 1/0469/15 and APVV-0050-11 (Slovakia).

References

[1] H. Song, S. A. Bass, U. Heinz, T. Hirano and C. Shen. Phys.Rev.Lett. 106, 192301, (2011).
[2] C. Nonaka and S. A. Bass, Phys.Rev. C75, 014902 (2007).
[3] P. Huovinen, P.F. Kolb, U. Heinz, P.V. Ruuskanen, and S.A. Voloshin, Phys.Lett. B503, 58-64 (2001).
[4] B. Schenke, S. Jeon, and C. Gale, Phys.Rev. C82, 014903, (2010).
[5] P. Huovinen, Nucl.Phys. A761, 296-312 (2005).
[6] T. Hirano and K. Tsuda, Phys.Rev. C66, 054905 (2002).
[7] Z. Qiu, C. Shen and U. Heinz, Phys.Lett. B707, 151-155 (2012).
[8] B. Schenke, S. Jeon, and C. Gale, Phys.Rev.Lett. 106, 042301 (2011).
[9] B. H. Alver, C. Gombeaud, M. Luzum, and J. Y. Ollitrault, C82, 034913 (2010).
[10] D. Teaney and L. Yan, Phys. Rev. C83, 064904 (2011).
[11] F.G. Gardim, F. Grassi, M. Luzum, J.-Y. Ollitrault, Phys. Rev. C85, 024908 (2012).
[12] H. Niemi, G.S. Denicol, H. Holopainen, P. Huovinen, Phys. Rev. C87, 54901 (2013).
[13] Ch. Gale *et al.*, Phys. Rev. Lett. 110, 012302 (2013).
[14] M. Schulc and B. Tomášik, Phys.Rev. C90, 064910 (2014).
[15] Y. Tachibana and T. Hirano, Phys. Rev. C90, 021902 (2014)
[16] R. P. G. Andrade, J. Noronha and G. S. Denicol, Phys. Rev. C90, 024914 (2014)
[17] J. Adams et al (STAR Collaboration), Phys. Rev. Lett.91, 072304 (2003).
[18] G. Aad et al (ATLAS Collaboration), Phys. Rev. Lett.105, 252303, (2010).
[19] S. Chatrchyan et al (CMS Collaboration), Phys. Rev. C84, 024906 (2011).
[20] K. Aamodt et al (ALICE Collaboration), Phys. Lett. B696, 30 (2011).
[21] L. M. Satarov, H. Stoecker and I. N. Mishustin, Phys. Lett. B627, 64, (2005).
[22] J. Casalderrey-Solana, E. V. Shuryak and D. Teaney, J. Phys. Conf. Ser.27, 22 (2005).
[23] V. Koch, A. Majumder and X. N. Wang Phys., Rev. Lett.96, 172302 (2006).
[24] M. Schulc and B. Tomášik, J.Phys. G40 (2013) 125104.
[25] B. Betz and M. Gyulassy, JHEP 1408, 090 (2014).
[26] T. Renk, Phys. Rev. C85, 044903 (2012).
[27] B. Schenke et al. Phys.Rev. C82, 014903 (2010).
[28] B. Schenke, S. Jeon and C. Gale, Phys.Lett. B 702 59 (2011).
[29] P. Petreczky, P. Huovinen, Nucl. Phys. A 897 26 (2010).
[30] B. Betz, J. Noronha, G. Torrieri, M. Gyulassy, I. Mishustin and D. H. Rischke, Phys. Rev. C 79, 034902 (2009).
[31] B. Betz, J. Noronha, G. Torrieri, M. Gyulassy and D. H. Rischke, Phys. Rev. Lett. 105, 222301 (2010).
[32] J. P. Boris, D. L. Book, J. Comp. Phys. 11, 38 (1973).
[33] C. R. DeVore, J. Comput. Phys. 92, 142 (1991).
[34] B. Betz, EPJ Web Conf. 13, 07002 (2011).
[35] B. Tomášik and P. Lévai, J. Phys. G 38 095101 (2011).
[36] F. Cooper and G. Frye, Phys. Rev. D 10, 186 (1974).
[37] M. Chojnacki, A. Kisiel, W. Florkowski and W. Broniowski, Comput. Phys. Commun. 183, 746 (2012).
[38] S. Floerchinger and U. A. Wiedemann, Phys. Lett. B 728, 407 (2014)
[39] S. Floerchinger and U. A. Wiedemann, Phys. Rev. C 88, 044906 (2013)
[40] B. Tomášik, Acta Phys. Polon. B **36** (2005) 2087 [nucl-th/0409074].
[41] M. Csanád, B. Tomášik and T. Csörgő, Eur. Phys. J. A **37** (2008) 111 doi:10.1140/epja/i2008-10605-7 [arXiv:0801.4434 [nucl-th]].

[42] S. Lökös, M. Csanád, T. Csörgő and B. Tomášik, arXiv:1604.07470 [nucl-th].
[43] A. Adare *et al.* [PHENIX Collaboration], Phys. Rev. Lett. **112** (2014) no.22, 222301 doi:10.1103/PhysRevLett.112.222301 [arXiv:1401.7680 [nucl-ex]].
[44] R. Kopečná and B. Tomášik, Eur. Phys. J. A **52** (2016) no.4, 115 doi:10.1140/epja/i2016-16115-1 [arXiv:1506.06776 [nucl-th]].
[45] I. Bouras, A. El, O. Fochler, H. Niemi, Z. Xu and C. Greiner, Phys. Lett. B **710**, 641 (2012) Erratum: [Phys. Lett. B **728**, 156 (2014)]
[46] I. Bouras, B. Betz, Z. Xu and C. Greiner, Phys.Rev. C 90, 2, 024904 (2014).
[47] K. Zapp, J. Stachel and U. A. Wiedemann, Phys. Rev. Lett. **103**, 152302 (2009)
[48] K. C. Zapp, Eur. Phys. J. C **74**, no. 2, 2762 (2014)
[49] K. C. Zapp, Phys. Lett. B **735**, 157 (2014)
[50] S. Floerchinger and K. C. Zapp, Eur. Phys. J. C **74**, no. 12, 3189 (2014)
[51] K. C. Zapp and S. Floerchinger, Nucl. Phys. A **931**, 388 (2014)